SECURITY INFORMATION

RESTRICTED UNCLASSIFIED

RM L52F04

NACA RM L52F04

NACA

FOR REFERENCE

NOT TO BE TAKEN FROM THIS ROOM

RESEARCH MEMORANDUM

LOW-SPEED INVESTIGATION OF THE EFFECTS OF NACELLES ON THE LONGITUDINAL AERODYNAMIC CHARACTERISTICS OF A 60° SWEPTBACK DELTA-WING - FUSELAGE COMBINATION WITH NACA 65A003 AIRFOIL SECTIONS

By William I. Scallion

Langley Aeronautical Laboratory
Langley Field, Va.

CLASSIFICATION CANCELLED

Authority J. W. Crowley ... 12/7/53 ... See NACA

E.O. 10501

By [illegible] 12/18/53

RA 1663

NATIONAL ADVISORY COMMITTEE
FOR AERONAUTICS

WASHINGTON
July 23, 1952

UNCLASSIFIED

RESTRICTED

1H NACA RM L52F04

NATIONAL ADVISORY COMMITTEE FOR AERONAUTICS

RESEARCH MEMORANDUM

LOW-SPEED INVESTIGATION OF THE EFFECTS OF NACELLES ON THE LONGITUDINAL AERODYNAMIC CHARACTERISTICS OF A 60° SWEPTBACK DELTA-WING - FUSELAGE COMBINATION WITH NACA 65A003 AIRFOIL SECTIONS

By William I. Scallion

SUMMARY

An investigation was conducted in the Langley full-scale tunnel to determine the effects of symmetrically located wing nacelles on the low-speed aerodynamic characteristics of a 60° sweptback delta-wing - fuselage combination. The model was tested with three spanwise nacelle locations (0.33 semispan, 0.50 semispan, and 0.66 semispan) with three chordwise positions at each spanwise station. The longitudinal aerodynamic characteristics were determined from force measurements and visual-flow observations at Reynolds numbers from 1.55×10^6 to 2.77×10^6 and Mach numbers from 0.07 to 0.12.

The most forward located midspan nacelle-model combination had the greatest reduction in maximum lift and all three midspan nacelle configurations were unstable in the high-lift range just prior to maximum lift. The least reduction in maximum lift was obtained from the outboard nacelle-model configurations and the model was stable through maximum lift for all three chordwise nacelle positions tested at that spanwise station. The nacelles considerably altered the separation vortex flow pattern over the basic model wing.

INTRODUCTION

The present trend of high-speed aircraft design toward thin delta wings has given rise to many problems associated with their physical and aerodynamic characteristics at high and low speeds. One of the problems created by the use of thin wing sections is the lack of internal storage capacity, which would require possible enlargement of the aircraft fuselage

to make up for the reduction of wing storage space. Another practical method of increasing storage space appears to be the attachment of external stores or engine nacelles to the wings of such aircraft.

As part of a program of investigation of the low-speed aerodynamic characteristics of thin delta wings in the Langley full-scale tunnel, the exploratory investigation reported herein deals with the effects of external stores or nacelles (hereinafter referred to as nacelles) on the low-speed characteristics of a 3-percent-thick, 60° sweptback delta-wing - fuselage combination. The fuselage and nacelles were considered to be representative of high-speed shapes currently under study. Force measurements of lift, pitching moment, drag, and flow studies were made through the angle-of-attack range for several chordwise and spanwise locations of the nacelles. A symmetrical location on the wing-chord plane was the only position in the vertical plane tested. Most of the force measurements were taken at a Reynolds number of 2.77×10^6.

COEFFICIENTS AND SYMBOLS

All results are presented in the standard NACA form of coefficients, and are referred to the wind axes. Moments are referred to the quarter-chord point of the mean aerodynamic chord.

C_L	lift coefficient, L/qS
C_D	drag coefficient, D/qS
C_m	pitching-moment coefficient, $M/qS\bar{c}$
R	Reynolds number, $\rho V\bar{c}/\mu$
μ	kinematic viscosity of air, slugs/ft sec
L	lift, lb
D	drag, lb
M	pitching moment, positive when moment tends to increase angle of attack, ft-lb
ρ	mass density of air, slugs/cu ft
q	free-stream dynamic pressure, $\frac{1}{2}\rho V^2$, lb/sq ft

[redacted]

V	free-stream velocity, ft/sec
S	total wing area, sq ft
c	wing chord measured parallel to plane of symmetry
$\bar{c}$	wing mean aerodynamic chord measured parallel to plane of symmetry, $\frac{2}{S}\int_0^{b/2} c^2 dy$, ft
y	distance along lateral axis, ft
b	wing span, ft
α	angle of attack of wing chord line, deg

MODEL AND TESTS

The model of this investigation had a delta-plan-form wing with 60° sweepback at the leading edge, an aspect ratio of 2.31, and an NACA 65A003 airfoil section. The wing was symmetrically located on the fuselage with the maximum thickness point of the fuselage $0.17\bar{c}$ ahead of the $0.25\bar{c}$ point of the wing. Coordinates for the fuselage, nacelles, and wing section are presented in tables I and II. The general arrangement and principal dimensions of the model, as well as the various nacelle positions investigated, are shown in figure 1. The nacelles were located at three spanwise stations $\left(0.33\frac{b}{2}, 0.50\frac{b}{2}, \text{and } 0.66\frac{b}{2}\right)$. There were also three chordwise positions at each spanwise station. The complete designation of a nacelle location was defined by the spanwise location in percent semispan and the chordwise location in inches between the rear end of the nacelle and the wing trailing edge. A symmetrical location on the wing-chord plane was the only vertical nacelle position tested.

The model was mounted on a sting balance for tests in the Langley full-scale tunnel as shown in figures 2 and 3. The model was tested on an alternate shift basis with the semispan wing model also shown in figure 3. All tests for the delta wing were conducted with the semispan model set at zero lift attitude, after detailed flow surveys made for this condition did not indicate any interference effects.

Force data (lift, pitching moment, and drag) were obtained through the angle-of-attack range from -3° to stall at zero yaw from a strain-gage balance mounted inside the model. Most of the force tests were made

at a Reynolds number of 2.77×10^6 based on the mean aerodynamic chord. Flow studies utilizing small wool tufts attached to the wing surface were also made throughout the angle-of-attack range at a Reynolds number of 2.28×10^6. In addition, visual studies were made of the influence of the nacelles on the vortex flow over the wing. These studies were made by moving a 4-foot wool streamer attached to a probe over the top surface of the wing.

The data are corrected for jet blockage. Calculations were made to determine the jet boundary and buoyancy corrections as applied to the model, but they were negligible and, therefore, were not applied. The data are uncorrected for an average stream angle of 0.2° and for the base drag of the model fuselage.

RESULTS AND DISCUSSION

In order that comparisons may be more readily made some of the force-test results are presented in summarized form in table III. Figure 4 shows the basic model characteristics at four Reynolds numbers ranging from 1.55×10^6 to 2.77×10^6 and figures 5, 6, and 7 present the lift, pitching moment, and drag characteristics of the model-nacelle combinations throughout the angle-of-attack range. Wing-flow diagrams are shown in figures 8 to 11 for the basic model and the model with three spanwise nacelle locations considered as representative of the other locations tested. Surface flow conditions are shown on the right wing and approximate vortex flow conditions are indicated on the left wing.

Basic Model

The lift curve of the basic wing-fuselage combination (fig. 4) was typical of that of a delta-wing configuration. The basic configuration attained a maximum lift coefficient of 1.23 at an angle of attack of approximately 32° and the lift-curve slope was approximately 0.05 per degree. The model was longitudinally stable through maximum lift and had a zero lift-drag coefficient of approximately 0.008.

For the Reynolds number range investigated (fig. 4), Reynolds number did not appreciably affect the results above a Reynolds number of approximately 1.84×10^6 and, even at the lowest values, very little effect was indicated for the lower lift (below $C_L = 0.7$) range.

Visual-flow studies (fig. 8) indicated that the general flow characteristics of the wing-fuselage combination were typical of the vortex-type flow previously observed (ref. 1) for sharp leading-edge delta wings.

Nacelles

Lift.- Adding the nacelles did not change the lift-curve slope of the basic model in the lower C_L range, but some of the nacelle installations did have sizeable effects on $C_{L_{max}}$. For the $0.33\frac{b}{2}$ and $0.50\frac{b}{2}$ nacelle configurations, the maximum lift coefficients were from approximately 0.10 to 0.13 lower than the basic model $C_{L_{max}}$ (table III) with the exception of the most forward nacelle position at the 0.50-semispan station. This configuration produced the largest reduction in $C_{L_{max}}$ (0.16) for any nacelle position investigated. The least detrimental nacelle location from the standpoint of $C_{L_{max}}$ was the $0.66\frac{b}{2}$ station. For this spanwise position the maximum lift values measured (fig. 7) were only approximately 0.04 below the value obtained for the basic model. The smaller reduction in maximum lift coefficients of the model with the $0.66\frac{b}{2}$ nacelle locations may be partially attributed to their location near the region of the wing tip. As shown in figure 8 this portion of the basic model wing stalls prior to maximum lift, and addition of the nacelles in this area would be expected to have little effect on maximum lift. Figures 8 to 11 show that the basic-wing stall pattern was least affected by this nacelle position.

Pitching moment.- In the low lift range (C_L = 0 to 0.4), the presence of the nacelles on the model generally decreased the longitudinal stability of the basic model but in no instance caused instability. At the higher lift coefficients (C_L = 0.4 to C_L = 0.8), longitudinal stability of the basic model was also decreased by the most forward-located nacelles, but moving the nacelles back along the chord progressively increased stability in every case, and the most rearward-located nacelle configurations were more stable than the basic model in this C_L range. For the one common longitudinal nacelle location tested (the rear ends of the nacelles 20 inches back of the wing trailing edge), the stability between C_L = 0 and C_L = 0.8 decreased as the nacelles were moved outboard.

The inboard and outboard nacelle configurations were longitudinally stable through $C_{L_{max}}$ with the exception that the $0.33\frac{b}{2}$ - 10 configuration became unstable at $C_{L_{max}}$ (fig. 5). Above C_L = 0.8 the midspan nacelles caused some degree of model instability between C_L = 0.9 and C_L = 1.05 for every longitudinal position investigated (fig. 6). The unstable breaks for this spanwise nacelle position appear to be the

result of premature stall of the entire tip region outboard of the nacelle as indicated in the flow diagram (fig. 10).

Visual-flow observations.- As indicated in figure 8 the probe test shows that the leading-edge separation vortex is formed at a low angle of attack. From the tuft diagram on figure 8 the intermittent transition of the leading-edge tufts from flow parallel to free stream to spanwise flow is also indicative of the formation of the separation vortex at low angles of attack. This vortex phenomenon is discussed more thoroughly in reference 1 for delta-type wings having sharp leading edges.

The flow characteristics of the model with nacelles at the $0.33\frac{b}{2}$ station are shown in figure 9. In this case the separation vortex formed outboard of the nacelle and, as the angle of attack was increased, the vortex swept back from the leading edge in the region of the wing tip in the same manner as on the basic model. Tufts placed inboard of the nacelle near its juncture with the leading edge indicated that the flow was very rough and that this portion of the wing stalled quite early ($\alpha = 12^\circ$).

With the nacelles installed at the $0.50\frac{b}{2}$ or $0.66\frac{b}{2}$ positions (figs. 10 and 11) a separation vortex formed at the leading edge inboard of the nacelles and a second vortex formed immediately outboard of the nacelles. The outboard vortices, although smaller, developed in the same manner as on the basic wing. On the $0.50\frac{b}{2}$ configuration the outboard vortex was not discernable after tufts indicated that portion of the wing had stalled ($\alpha = 21^\circ$). On both the $0.50\frac{b}{2}$ and $0.66\frac{b}{2}$ configurations, there was no visible evidence at low angles of attack that the inboard vortex continued over the nacelle. As the angle of attack was increased, it became apparent that the vortex was turned downstream just inboard of the nacelle. The effect of the nacelles on the outward vortex flow appeared to be similar to that of a fence and it is probable that the flow is influenced by a pressure gradient over the nacelle near the wing leading edge similar to that shown in reference 2.

SUMMARY OF RESULTS

The results of the low-speed investigation of the longitudinal aerodynamic characteristics of a 60° sweptback delta-wing - fuselage combination as affected by nacelles at various positions on the wing may be summarized as follows:

[redacted]

1. The basic wing-fuselage maximum lift coefficient was only slightly reduced by the 0.66-semispan-station nacelles, and from the standpoint of maximum lift coefficient this was the most favorable nacelle location. The largest reduction in maximum lift coefficient was obtained from the most forward-located nacelle at the midsemispan station.

2. The nacelles increased the longitudinal stability of the basic model in several instances in the higher lift range (C_L = 0.4 to C_L = 0.8). The outboard nacelle-model combinations were stable through the maximum lift coefficient at all three chordwise positions. The midspan nacelle-model combinations showed some degree of instability at the higher lift coefficients for every chordwise position tested.

3. The vortex pattern over the wing was altered by the nacelles. Two separation vortices were formed at the wing leading edge, one inboard and one outboard of the nacelle. The inboard vortex was turned downstream by the nacelle and remained inboard between the nacelle and fuselage.

Langley Aeronautical Laboratory
National Advisory Committee for Aeronautics
Langley Field, Va.

REFERENCES

1. May, Ralph W., Jr., and Hawes, John G.: Low-Speed Pressure-Distribution and Flow Investigation for a Large Pitch and Yaw Range of Three Low-Aspect-Ratio Pointed Wings Having Leading Edge Swept Back 60° and Biconvex Sections. NACA RM L9J07, 1949.

2. Hieser, Gerald, and Whitcomb, Charles F.: Investigation of the Effects of a Nacelle on the Aerodynamic Characteristics of a Swept Wing and the Effects of Sweep on a Wing Alone. NACA TN 1709, 1948.

[redacted]

TABLE I

COORDINATES OF FUSELAGE AND NACELLES

Fuselage ordinates

Station	x, in.	y, in.
0	0	0
1	.72	.333
2	1.08	.4284
3	1.80	.6156
4	3.60	1.040
5	7.20	1.735
6	10.80	2.322
7	14.40	2.838
8	21.60	3.733
9	28.80	4.449
10	36.00	4.989
11	43.20	5.387
12	50.40	5.662
13	57.60	5.850
14	64.80	5.965
15	72.00	6.001
16	79.20	5.947
17	86.40	5.794
18	93.60	5.466
19	100.80	5.128
20	108.00	4.789
21	115.20	4.453
22	120.00	4.224

Nose radius = .072

Nacelle ordinates

Station	x, in.	y, in.
0	0	0
1	.279	.195
2	.921	.471
3	2.315	.937
4	3.170	1.364
5	5.106	1.735
6	6.500	2.084
7	7.198	2.232
8	8.252	2.444
9	10.002	2.717
10	13.503	3.083
11	17.005	3.320
12	20.51	3.459
13	24.00	3.501
14	46.95	3.501
15	49.86	3.451
16	52.77	3.334
17	55.67	3.144
18	58.58	2.871
19	61.48	2.536
20	64.39	2.142
21	67.29	1.719
22	67.65	1.668

Nose radius =0.139

TABLE II

NACA 65A003 AIRFOIL ORDINATES

Station, percent chord	y, percent chord
0	0
.5	.234
.75	.284
1.25	.362
2.50	.493
5.00	.658
7.50	.796
10.00	.912
15.00	1.097
20.00	1.236
25.00	1.342
30.00	1.420
35.00	1.472
40.00	1.498
45.00	1.497
50.00	1.465
55.00	1.402
60.00	1.309
65.00	1.191
70.00	1.053
75.00	.897
80.00	.727
85.00	.549
90.00	.369
95.00	.188
100.00	0

TABLE III

SUMMARY OF RESULTS

Configuration	$C_{L_{max}}$	dC_m/dC_L (C_L = 0 to 0.4)	dC_m/dC_L (C_L = 0.4 to 0.8)	L/D (C_L = 1.0)	α^o (C_L = 1.0)	Remarks
Basic model	1.23	-0.094	-0.059	2.79	21.2	Stable
33-10	1.11	-0.045	-0.034	2.24	24.3	Unstable at $C_{L_{max}}$
33-15	1.10	-0.057	-0.055	2.20	25.2	Stable
33.20	1.10	-0.071	-0.064	2.09	25.2	Stable
50-15	1.07	-0.039	-0.034	2.09	26.0	Unstable (C_L 0.85-1.05)
50-20	1.12	-0.049	-0.050	2.20	24.9	Unstable (C_L 0.9-1.08)
50-25	1.13	-0.060	-0.079	2.52	22.8	Unstable (C_L 0.97-1.05)
66-20	1.20	-0.041	-0.047	2.61	21.6	Stable
66-25	1.19	-0.055	-0.074	2.59	21.8	Stable
66-30	1.20	-0.062	-0.082	2.74	21.0	Stable

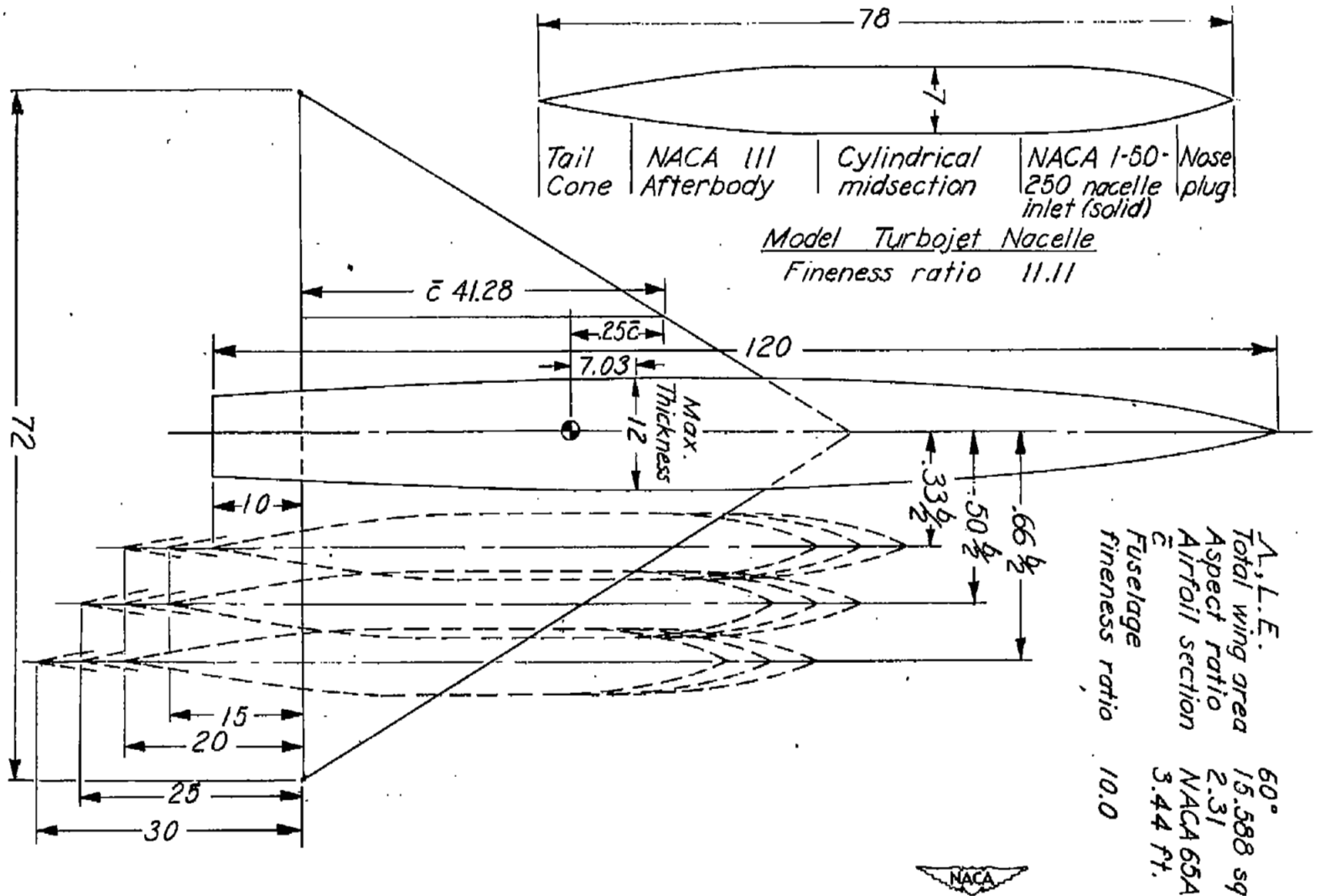

Figure 1.- General arrangement and principal dimensions of the 60° delta-wing model. All dimensions are given in inches.

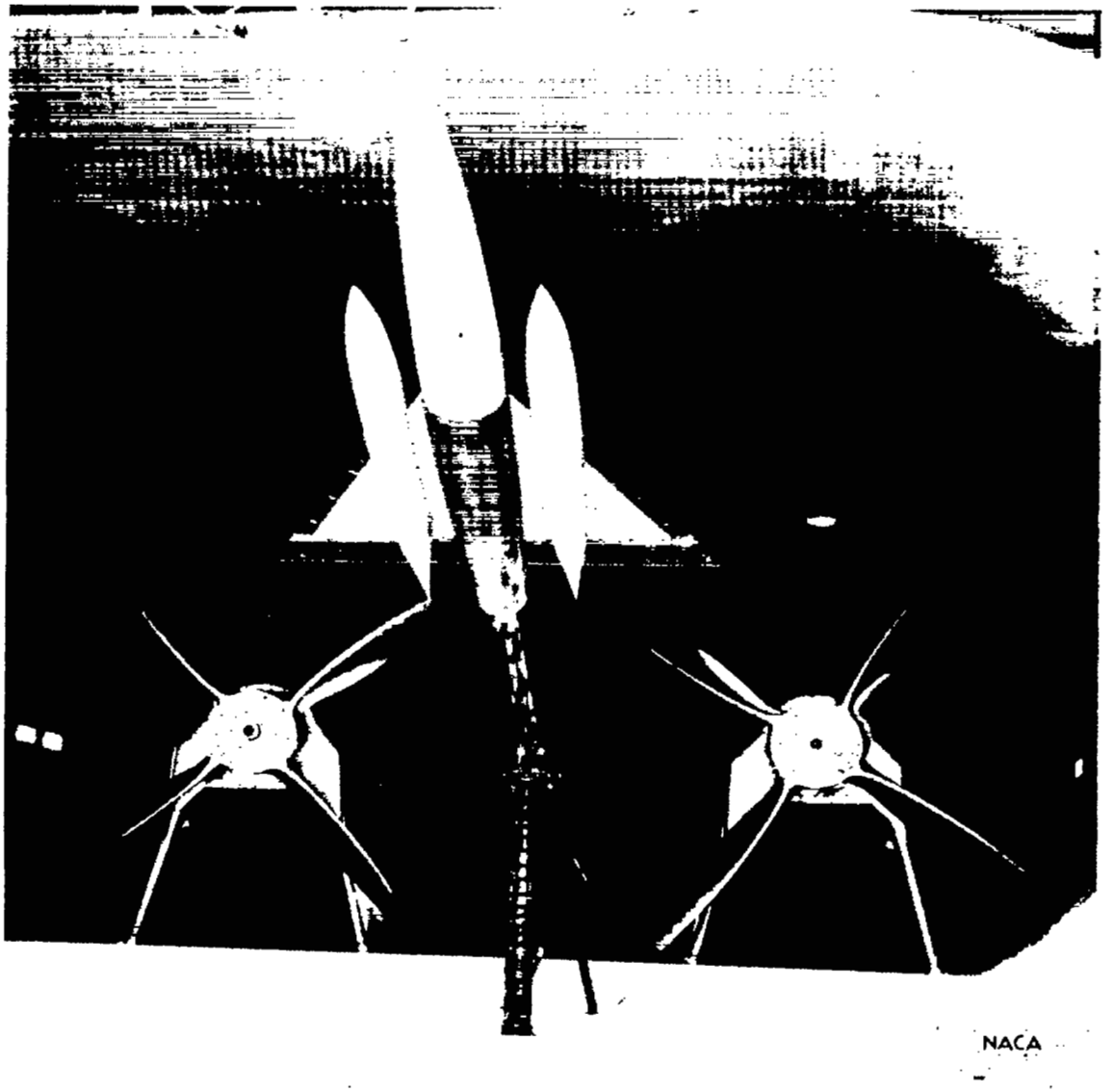

Figure 2.- Photograph of the 60° delta-wing model as mounted in the Langley full-scale tunnel.

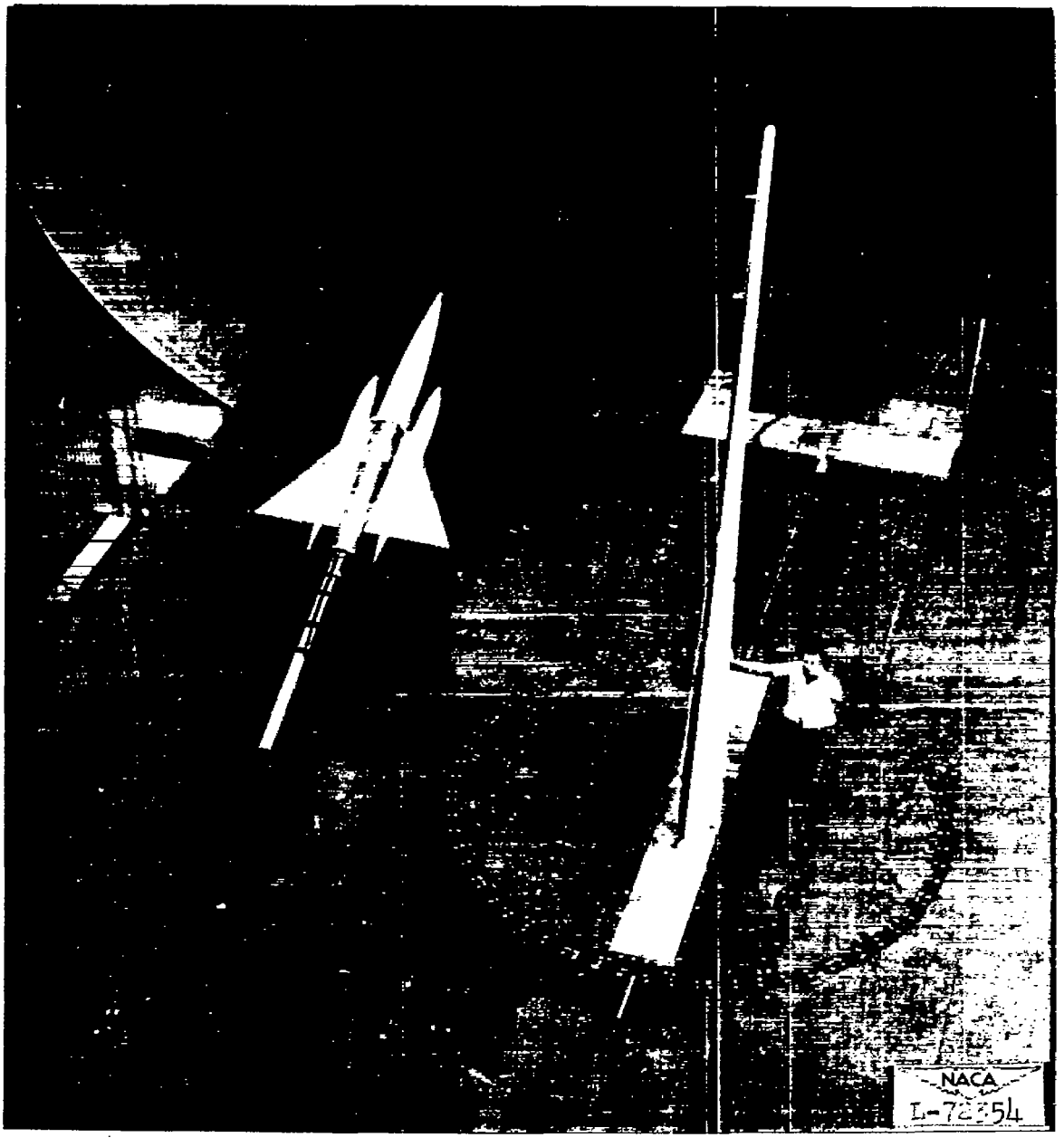

Figure 3.- General view of the 60° delta-wing model mounted in the Langley full-scale tunnel.

[redacted]

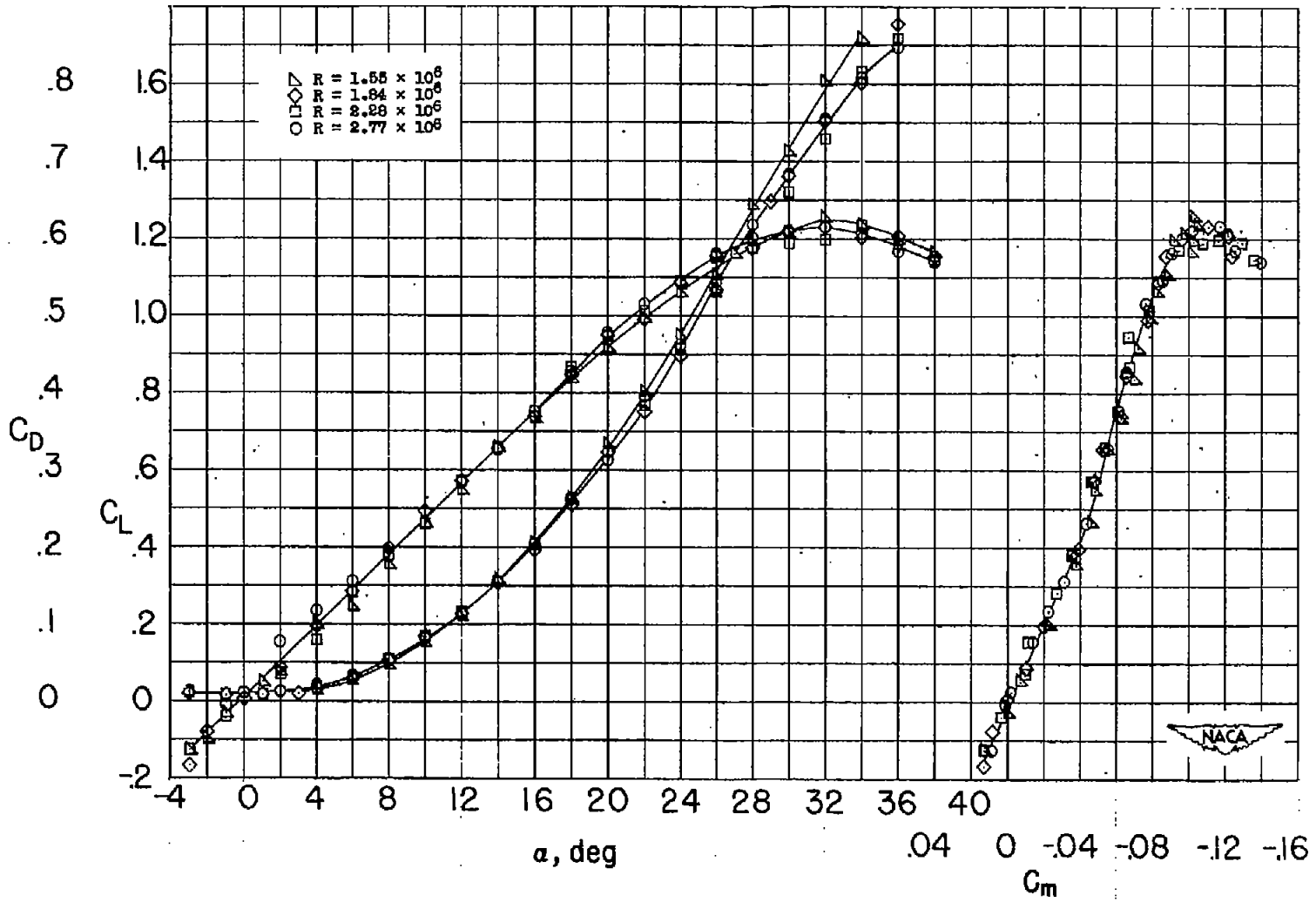

Figure 4.- Aerodynamic characteristics of the 60° delta-wing - fuselage combination.

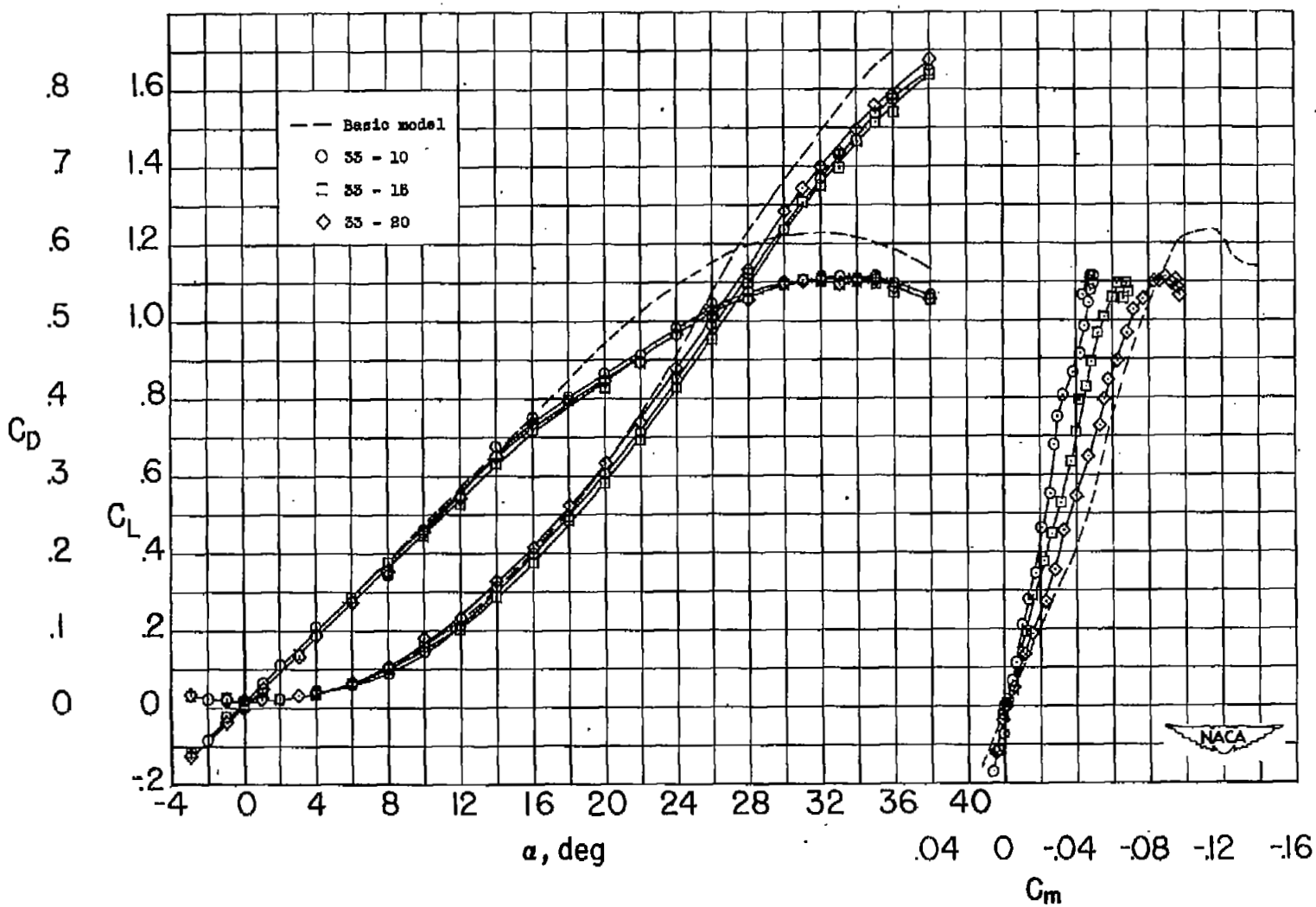

Figure 5.- Aerodynamic characteristics of the model with nacelles installed at the $0.33\frac{b}{2}$ station. $R = 2.77 \times 10^6$.

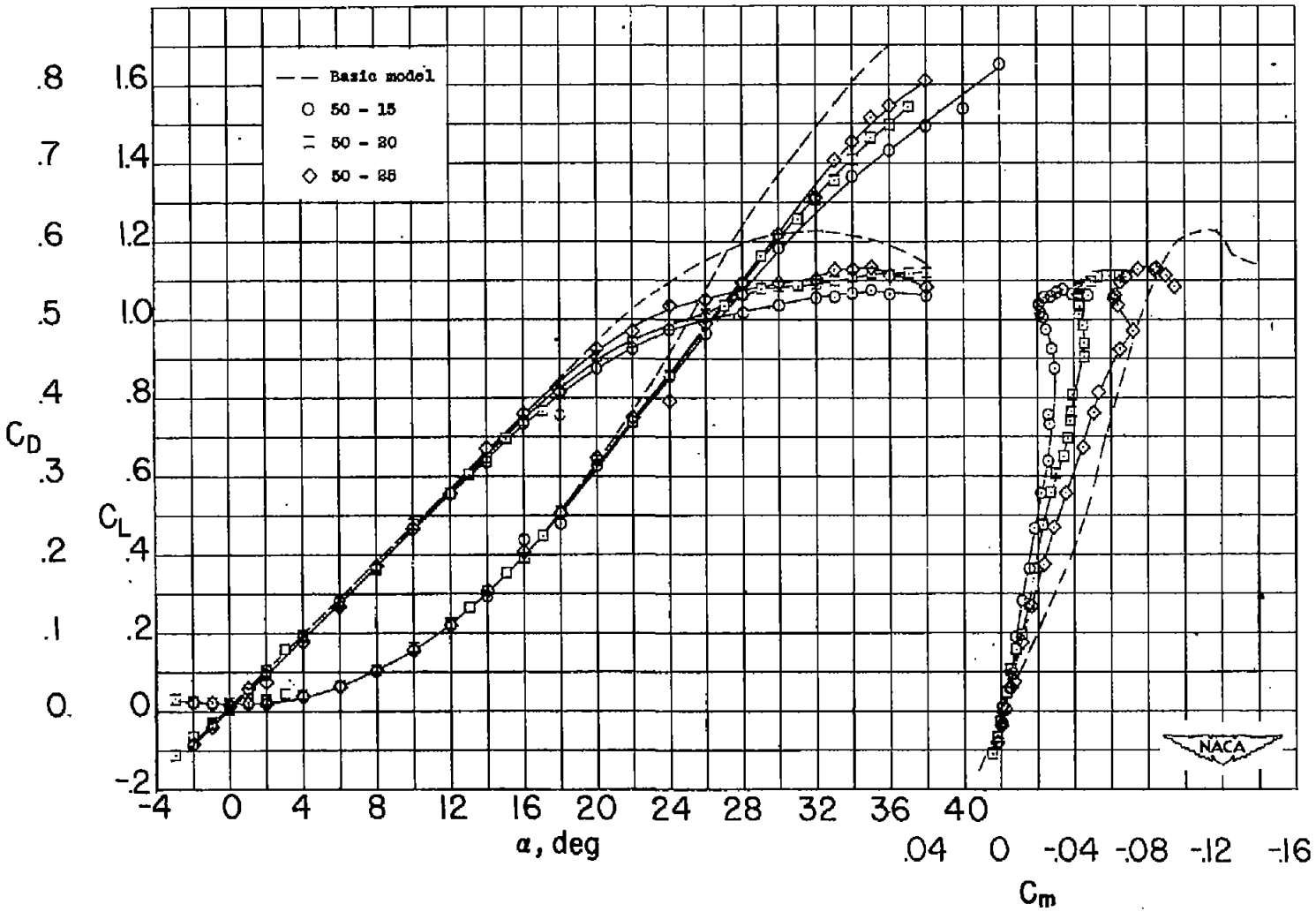

Figure 6.- Aerodynamic characteristics of the model with nacelles installed at the $0.50\frac{b}{2}$ station. $R = 2.77 \times 10^6$.

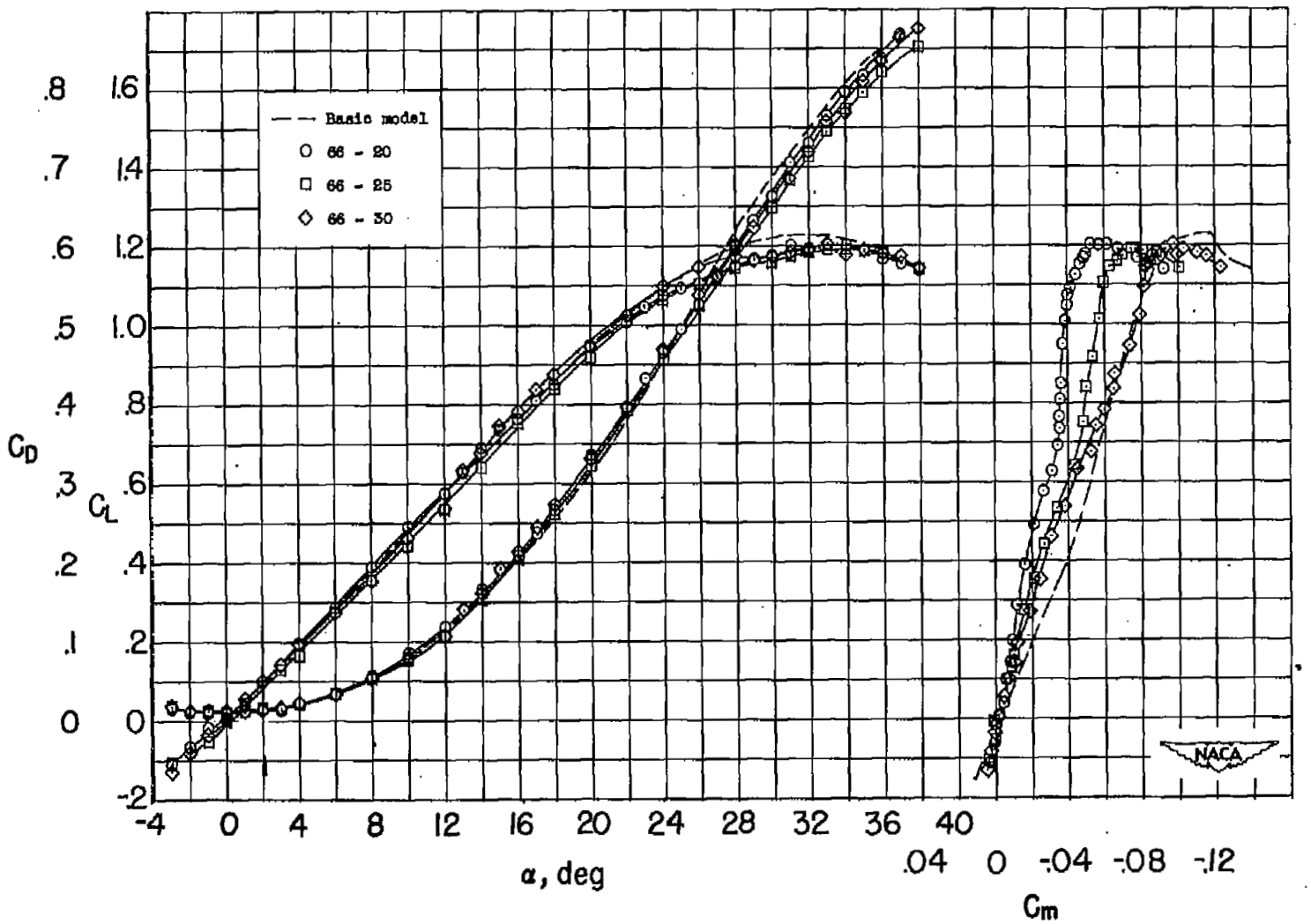

Figure 7.- Aerodynamic characteristics of the model with nacelles installed at the $0.66\frac{b}{2}$ station. $R = 2.77 \times 10^6$.

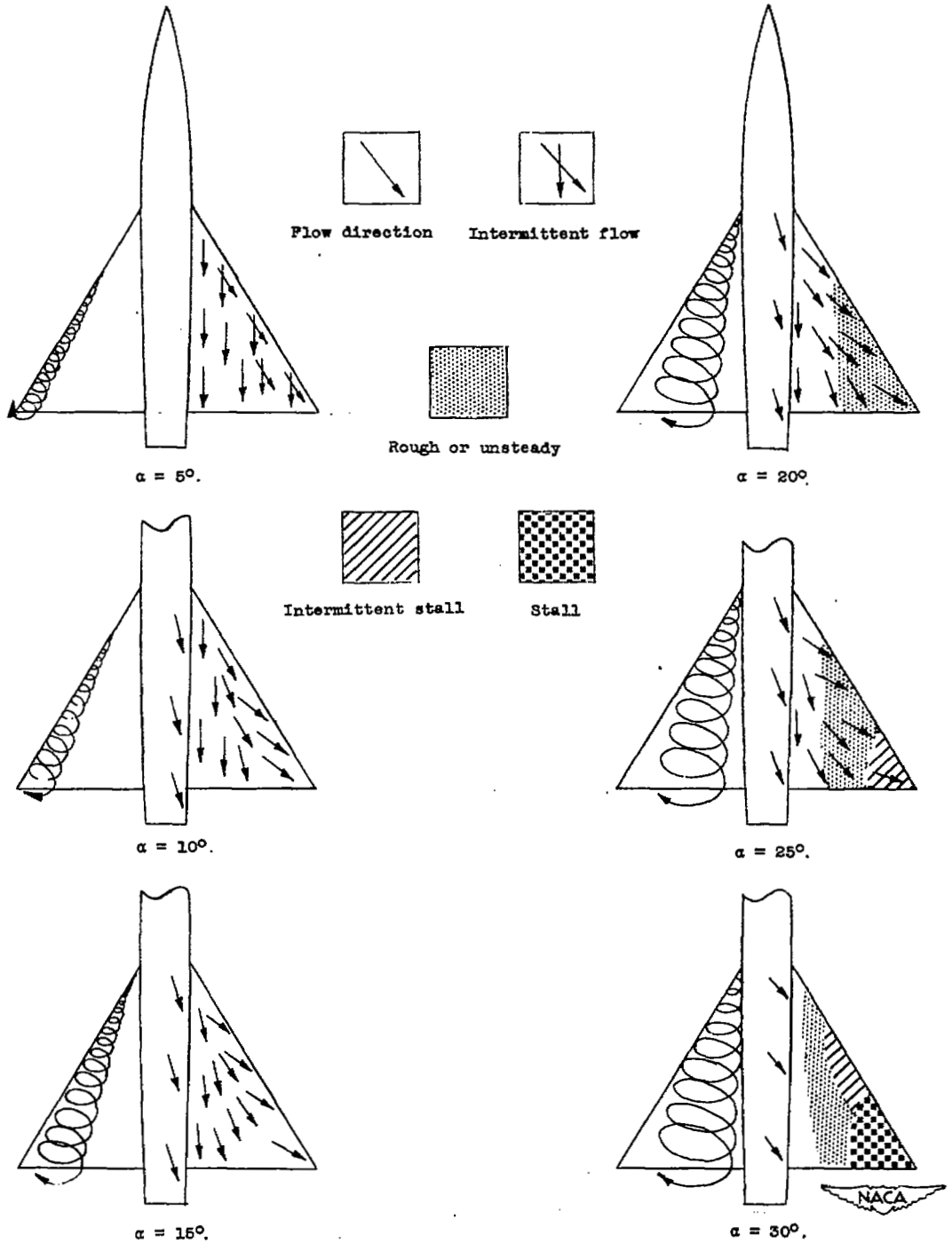

Figure 8.- Flow characteristics of the basic wing-fuselage combination.

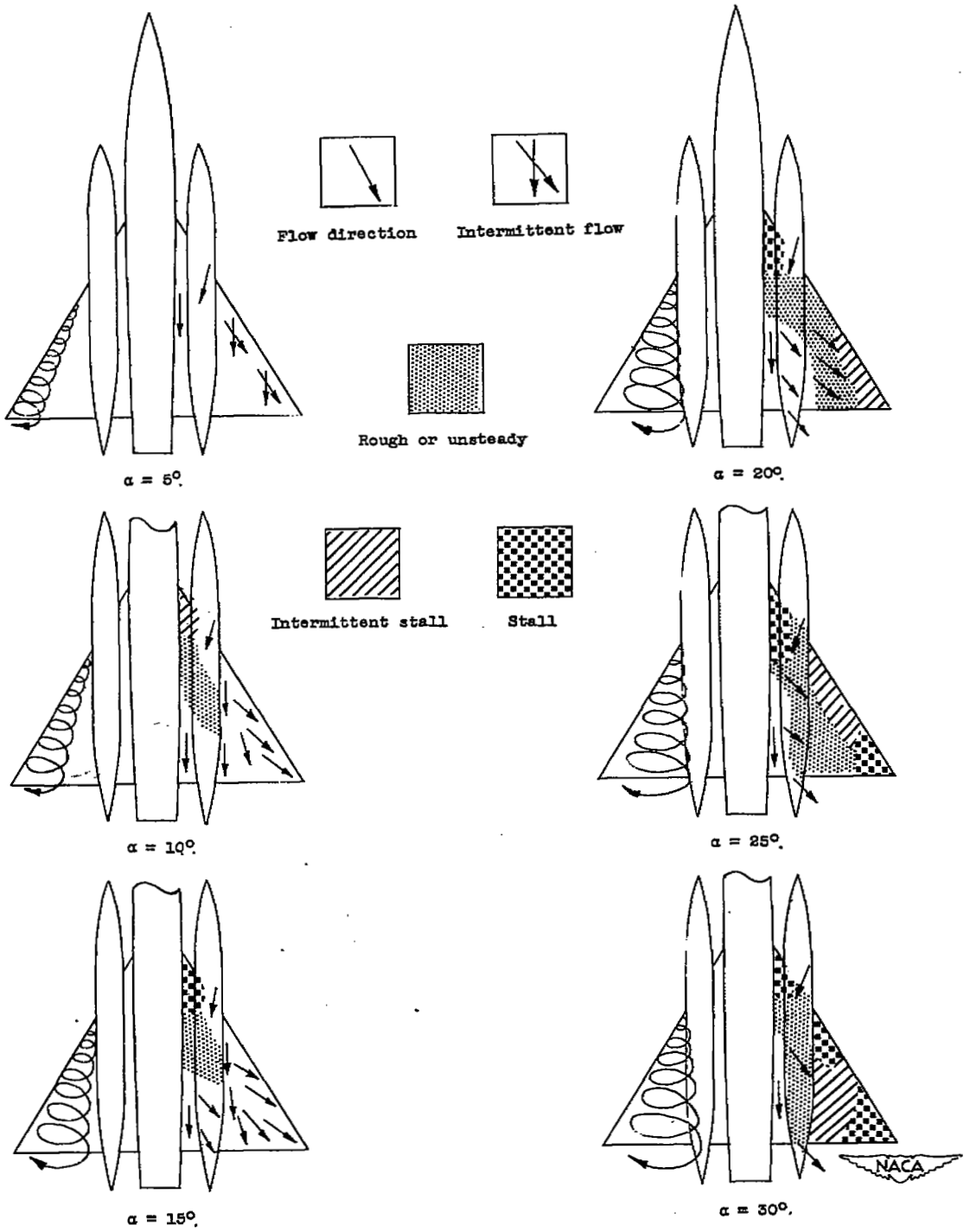

Figure 9.- Flow characteristics of the model with nacelles at the $0.33\frac{b}{2}$ - 10 station.

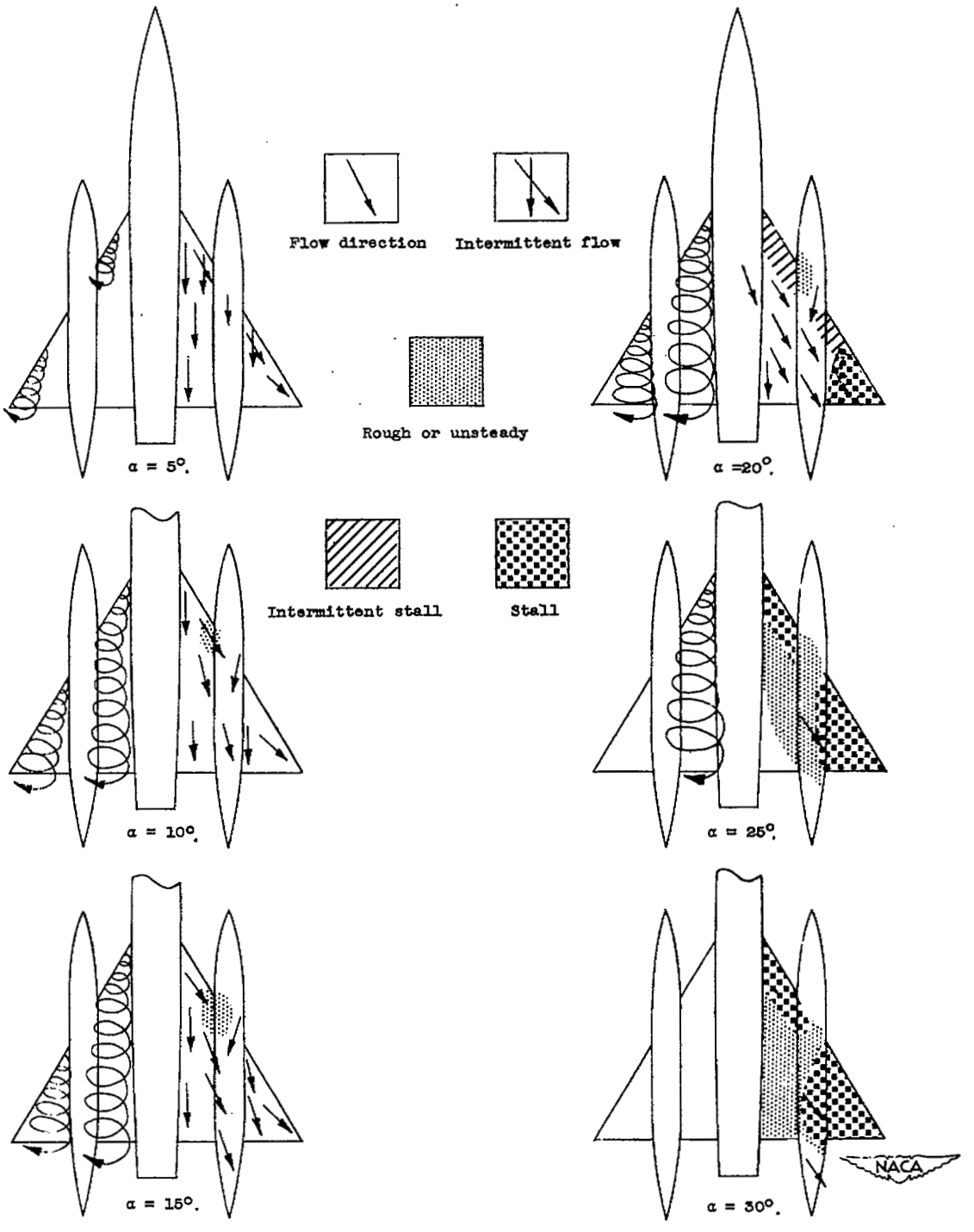

Figure 10.- Flow characteristics of the model with nacelles at the $0.50\frac{b}{2}$ - 20 station.

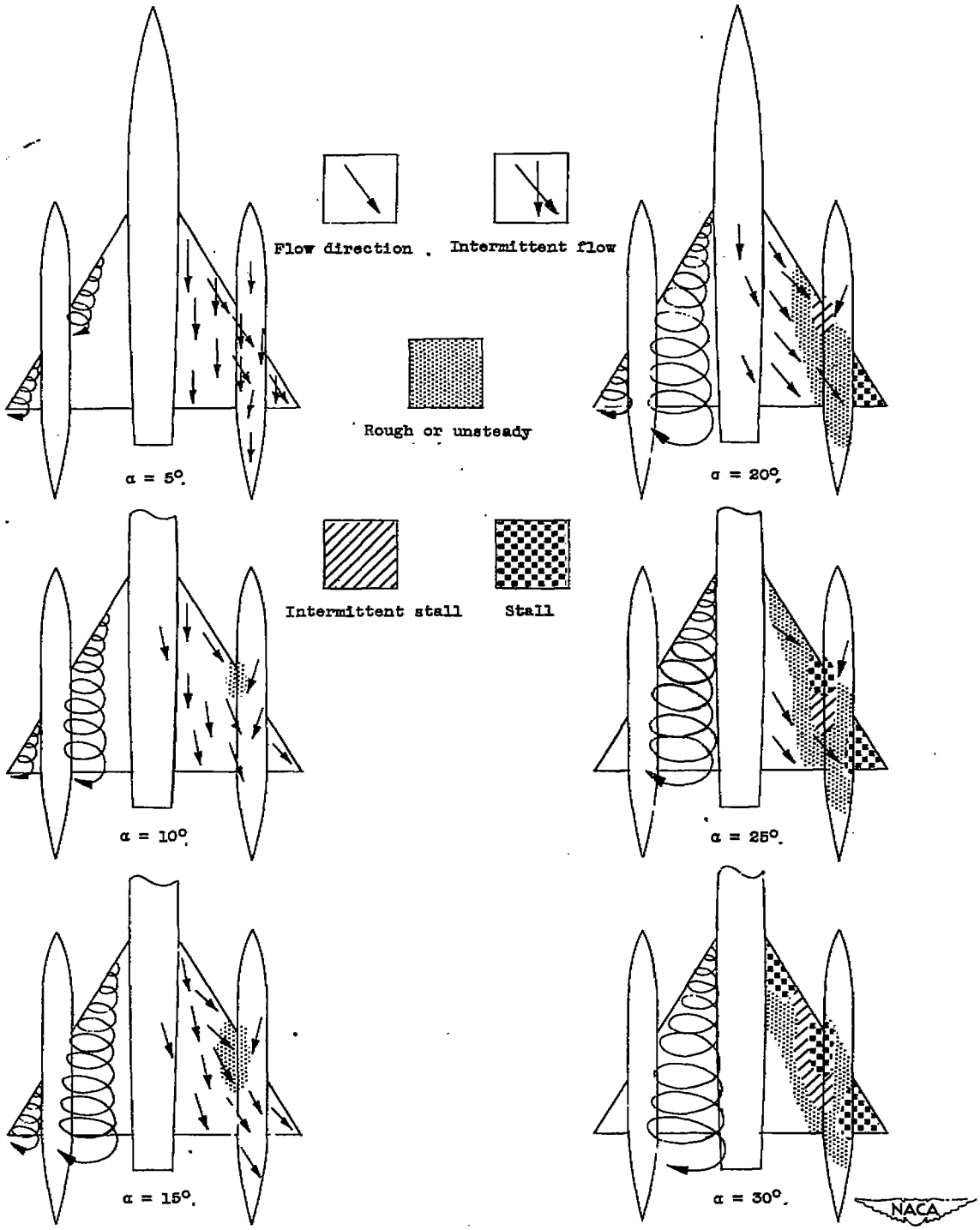

Figure 11.- Flow characteristics of the model with nacelles at the $0.66\frac{b}{2}$ - 20 station.

[redacted]

NACA-Langley - 7-23-52 - 350